A Novel Closed Loop Topology for Coupled Inductor Based DC-DC Converter

Srinivas Singirikonda, Member of IEEE,

Gargi Desai, Member of IEEE,

Abstract— In the closed loop topology for a coupled inductor based DC-DC converter we have a tendency to introduce a voltage multiplier converter with coupled inductance for high gain output charging the battery of a feedback loop for DC machine drive for variable input voltage. The dual switches structure is helpful to scale back the voltage stress and current stress of the switch. Additionally, 2 multiplier capacitors are charged throughout the switch-on period and switch-off period, which will increase the voltage conversion gain. Meanwhile, the energy stored within the inductance is recycled with the clamped capacitors. Thus, 2 main power switches with low on-resistance and low current stress are available. This project illustrates the operation principle of the designed DC-DC converter, the output voltage of the high step-up converter is maintained constant by automatic variation of the duty ratio with feedback as PI Controller. The constant output voltage for varying input DC voltage is represented graphically using MATLAB simulation for various industrial applications.

Index Terms — Dual switches, high step-up converter, switched capacitor, three-winding coupled inductor, closed loop, duty ratio, PI controller.

1 INTRODUCTION

NOWADAYS, due to the energy usage and atmosphere pollution, the renewable energy is widely used. The renewable energy sources like fuel cells and other PV cells generate low voltage output. Thus, high the step-up dc/dc converters are widely used for renewable energy systems [1]-[7]. In recent years several novel high step-up converters are developed. The system can convert the voltages from PV cells source into the high voltage via high step-up boost converter and then the renewable energy is transmitted to the load and utility through the inverter. Hence, the high step-up converter is essential.

In order to achieve the high step-up gain, the conventional step-up converters, such as the boost converter and flyback converter can be used to fulfil the high step-up requirement. In the recent years, the many high step-up converters have been developed. Despite the advances, the current and voltage stress of the power switch in high step-up single switch converters are larger, large conduction losses which cannot be avoided and the duty ratio variation is manually varied. However the voltage converter gain is limited in high step-up applications. Hence, based on the mentioned considerations, modifying a conventional dual switches converter which is an open loop system to a closed loop converter is suitable method.

The closed loop system is used to control the output voltage to a constant value for variable input voltages using PI controller. The voltage conversion ratio remains high, thus making the converter more suitable for step up dc-dc power conversion. The converter is simulated using MATLAB. Output levels are obtained as per the designed values for both converter (Open loop and closed loop) operations. Simulation results convey the operability of the dual switch converter with coupled inductor and voltage multiplier cell in closed loop system.

In the closed loop system with PI controller the output voltage is as the desired voltage and the duty ratio of the switches vary automatically as the input voltage changes maintaining the output voltage constant (i.e., 200V or 360V).

The dc-dc converters with high step-up voltage gain are widely used for many applications like lasers, fuel cells energy

conversion systems, solar cell energy conversion system, X-ray systems and high intensity-discharge lamp ballasts for automobile headlamps. Theoretically, a dc-dc boost converter achieves high voltage gain with extremely high duty ratio. However, in practice, the step-up voltage gain is limited due to the effect of power switches, rectifier diodes, and the series resistance of inductors and capacitors.

The classical boost converter with non-isolated dc-dc operation can provide high step-up voltage gain along with the penalty of high voltage and current stresses, high duty cycle operation and dynamic response. When operating with high current and voltage levels, the efficiency can be reduced by the diode reverse recovery current. Among the few non-isolated dc-dc converters achieve high static gain, as the quadratic boost converter, but additional filter capacitors and inductors should be used and the switch voltage is high. A new alternative for the implementation of high step-up structures is proposed in the step-up converter with the use of the voltage multiplier cells integrated with classical non-isolated dc–dc converters. The uses of the voltage multiplier in the classical dc–dc converters add new operation characteristics, becoming the resultant structure well suited to implement high-static gain step-up converters [9]. The novel non-isolated dc-dc to converter with high voltage gain based on three-state switching cell and voltage multiplier cells, this topology has the advantages of input current is continuous with low ripple, input inductor is designed for twice the switching frequency, with consequent volume and weight reduction; the voltage stress across the switches is lower than half of the output voltage, and naturally clamped by one output filter capacitor. As a disadvantage, a small snubber is necessary for each switch and one additional winding per cell is required for the autotransformer.

Later, in [7] the high step-up dc-dc converter for the applications of AC Photovoltaic module design includes a floating switch to isolate the PV panel when the ac module is off to interrupt the energy conversion from PV panel to the ac module. Here, the operating modes include two modes of operation continuous conduction mode (CCM) and discontinuous conduction mode (DCM) where in the coupled inductor based dc-dc converter there is only CCM which makes the studies of the switching waveforms flexible. The turns ratio of the coupled inductor and duty ratio are not extremely varied which results in high output voltage conversion, the energy of the leakage coupled inductor is recycled to the load efficiently. In the conversion of energy and safety perspective it has been designed to operate only when the ac module is on and this high step-up converter is isolated when it is off.

Then, an [13] interleaved high step-up converter with built-in voltage multiplier cell transformers for the application of sustainable energy for the voltage gain conversion was implemented with a turns ratio of 14:14 for the optimization of switch duty ratio. Here, the built-in transformer voltage multiplier cells helps to avoid extreme duty ratio in the interleaved boost converter, hence the power level is also increased. But here due to the transformer turns ratio the losses are more hence the circuit configuration also gets complicated.

In a dual switch DC-DC converter with charge pump and three-winding coupled inductor [11], high voltage gain and efficiency is obtained which is similar circuit as the coupled inductor based converter and the operation is performed on open-loop and there is no control over the output voltage.

2 CONTROL STRATEGY

The PI controller is employed to achieve the constant DC output voltage by controlling the pulse width with the variable DC supply. Here, the converter consists of two active switches, five diodes and five capacitors. The two switches share same operation signal and one control circuit is needed. The variable input voltage is given as the source with the help of PV panel, a constant output voltage is same as the reference value and the error is fed back to the PI Controller generating duty ratio which is varied automatically.

The equivalent circuit model of the three-winding coupled electrical device includes the magnetizing inductance lumen, the leakage inductance L_k, and a perfect electrical device with primary N_1 turns and 2 secondary windings N_2 and N_3 . The converter device consists of 2 active switches, 5 diodes, and 5 capacitors. The switches S_1 and S_2 share a similar operation

signal and one feedback loop is required. The discharge electrical device energy of the coupled electrical device is recycled to the capacitors C_1 and C_2, and therefore the voltage spikes on the switches are significantly reduced. This makes low conducting resistance R_{ds}(on) of the switches out there. Thus, the efficiency is upgraded and therefore the high conversion gain will be achieved.

The objective of the novel closed loop topology for coupled inductor based DC-DC converter is to perform operation of the converter with PI controller which compares the reference value and the error is fed to it generation dynamic duty ratio. This duty ratio is automatically varied wherein in previous studied it is varied manually in open loop system.

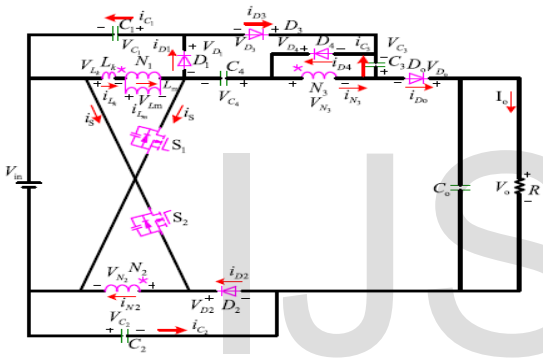

Fig.1 Circuit Configuration

The operation of the converter with PI Controller is studied in continuous conduction mode (CCM) and the modes of operation are analyzed in detail. The eight operating modes are described as follows.

To alter the circuit analysis of the converter, the subsequent assumptions are made, the voltages across the capacitors C_3 and C_4 will be adjusted by the turns ratio of the coupled inductor.

1) The Capacitors C_1, C_2, C_3, C_4, and C_o square measure giant enough; so, V_{C1}, V_{C2}, V_{C3}, V_{C4}, and V_o square measure thought to be constant values;

2) The ability devices square measure ideal, however the parasitic capacitors of the switches square measure considered;

3) The coupling coefficient of the coupled inductor k is equal to $L_m/(L_m+L_k)$, the turns ratio is $N_1 : N_2 : N_3 = 1:1: N$. The primary winding with N_1 turns, two secondary windings with N_2 and N3 turns of the ideal transformer are, respectively, represented by L_1, L_2 and L_3 ($L_1 : L_2 : L_3 = 1:1: N_2$).

2.1 Operation of Voltage Multiplier Converter

The operating principles for the continuous conduction mode (CCM) are analyzed in detail herein. The eight operating modes are described as follows.

CCM Operation

Mode I [t0, t1]: During the transition interval, the switches S_1 and S_2 begin to conduct. Diodes D_1, D_2, D_3, and D_o are reverse biased. Diode D_4 is forward biased. The current flow is as shown in Fig.2. The outpouring inductance L_k and magnetizing inductance Lm are charged by the input supply V_{in}. The inductance L_2 is additionally charged by the input supply. The L_2 inductance current i_{Lk} will increase linearly. Because of the leakage inductance, the inductance current i_{L3} and diode current i_{D4} decrease slowly. Therefore, the voltage of diode D_3 is clamped by input supply V_{in}, clamped voltages V_{C1} and V_{C4}; the voltage of diode D_o is clamped by voltages V_{C3}, V_{C4}, and V_{C2}. The voltage steps are generally formed. The output Co provides the energy to load R and the current i_{D4} becomes zero (i.e., sort = i_{Lm}), this operative mode ends.

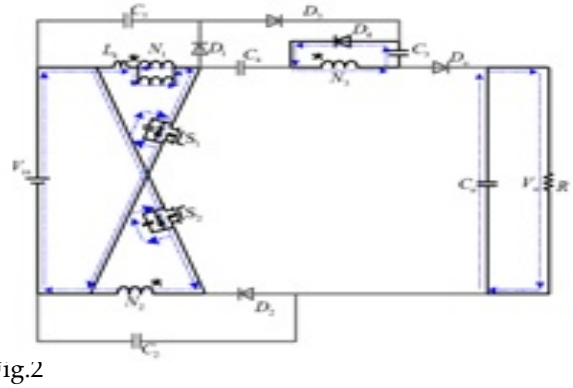

Fig.2

Mode II [t_1, t_2]: During the transition interval, the switches are still turned on. Diode D_3 is forward biased. Diodes D_1, D_2, D_4, and D_o are reverse biased. The current flow path is shown in Fig. 3.

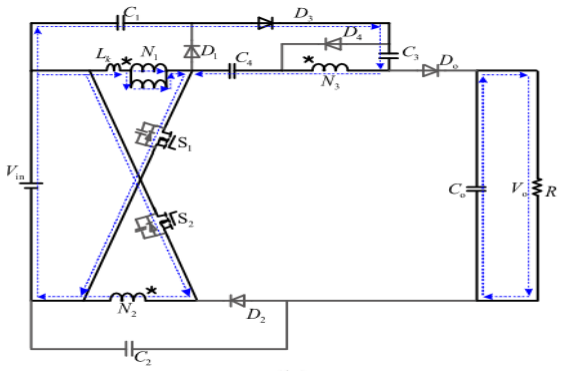

Fig.3

The magnetizing inductance L_m and inductance L_2 are charged in parallel by the input supply V_{in}. The energy from the input supply V_{in} transfer to the inductance L_3 to C_4 with the input supply V_{in}, clamped voltages V_{C1}, V_{C3} along. The output capacitor C_o provides the energy to load R. once the switches square measure turned off at t = t_2, this interval is finished.

Mode III [t2, t3]: In this transition interval, the switches are turned off. Diodes D_1, D_2, D_4, and D_o are reverse biased. Fig.4 shows the current-flow path. The energies of the leakage inductance L_k and magnetizing inductance L_m are released to the parasitic capacitors of the switches, respectively. The blocking capacitor C_4 is still charged. The output capacitor C_o provides the energy to load R. When the diodes D_1 and D_2 are forward biased at t = t_3, this operating mode ends.

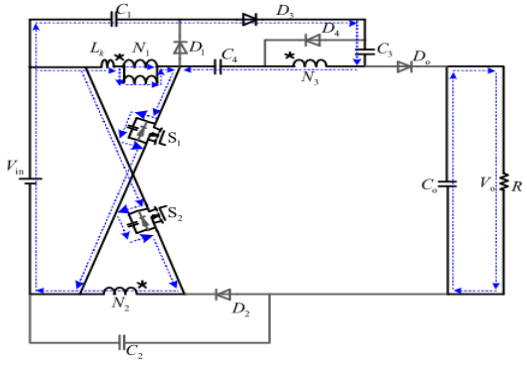

Fig.4

Mode IV [t_3, t_4]: In this transition interval, the switches are turned off. Diodes D_1, D_2, and D_3 are forward biased. Diode D_o is reverse biased. Fig. 5 shows the current-flow path.

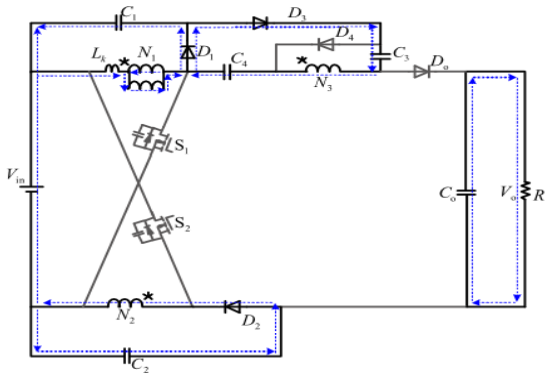

Fig.5

The energies of the leakage inductance L_k and magnetizing inductance L_m are released to the clamped capacitor C_1 and energy of the inductor L_2 is transferred to the clamped capacitor C_2. The blocking capacitor C_4 keeps charging. In addition, due to the leakage inductance, and the diode current i_{D3} keeps flowing though diode D_1; therefore, the voltage across the diode D_4 is clamped by the blocking voltage V_{C4}. The output capacitor C_o provides the energy to load R. When the currents i_{D3}, i_{C3}, and i_{L3} decrease to zero at t = t_4, this operating mode ends.

Mode V [t_4, t_5]: In this transition interval, the switches are turned off. Diodes D_1, D_2, and D_o are forward biased. Diodes D_3 and D_4 are reverse biased. The current-flow path is shown in Fig.6**.**

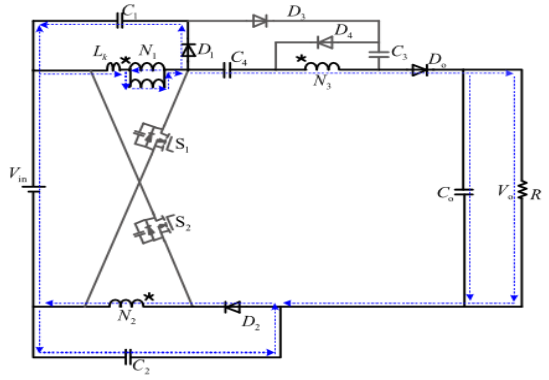

Fig.6

The energies of the leakage inductance L_k and the magnetizing inductance L_m are released to the clamped capacitor C_1 and the energy of inductor L_2 is transferred to the clamped capacitor C_2. The diode current i_{Do} increases almost at a constant slope. The input source V_{in}, three-winding coupled inductor, and the blocking voltage V_{C4} are connected in series to charge the output capacitor C_o and provide

energy to the load R. When the diode current i_{Do} is equal to diode current i_{D2} (i.e., capacitor current decreases to zero) at t = t_5, this operating mode is finished.

Mode VI [t_5, t_6]: In this transition interval, the diodes D_1, D_2 and D_o are forward biased during the switches turned off and the D_3 and D_4 are in reverse bias. The flow of current is shown in Fig.7. It is almost same as Mode V but the capacitor C_2 is discharged. This operating mode ends at t=t_6, D_4 is forward biased at this time of interval.

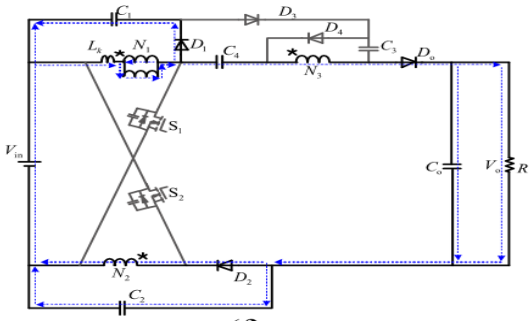

Fig.7

Mode VII [t_6, t_7]: In this transition interval, Diodes D_1, D_2, D_3 and D_0 are in forward bias only D_4 is in reverse bias during the switch off mode. The flow of current is shown in Fig.8.

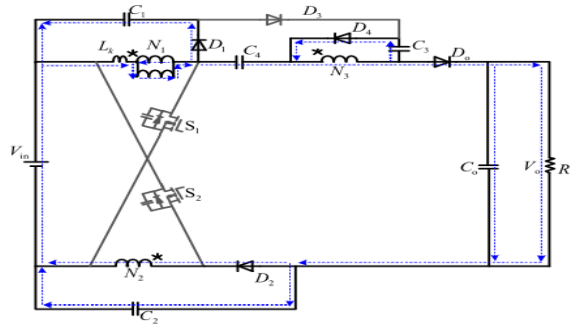

Fig. 8

The leakage and magnetizing inductance releases the energies to clamped capacitor C_1. The parallel connection of the inductor L_2 and capacitor C_2 discharges the energies to the load and output capacitor C_o. Simultaneously, the input V_{in}, L_1, L_2 and the blocking voltage V_{C4} provides the energy to the output capacitor C_o and load R. The i_{Do} drops almost a constant slope. In addition, the energy of the inductor L_2 is transferred to the capacitor C_3 while the diodes currents i_{D1} and i_{D2} are equal to zero t=t_7 in this mode.

Mode VIII [t_7, t_8]: In this transition interval, the switches are turned off. Diodes D3 and Do are forward biased. Diodes D_1, D_2, and D_4 are reverse biased. The current-flow path is shown in Fig.9

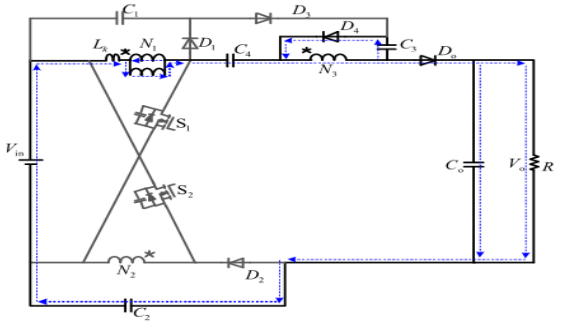

Fig.9

The leakage inductance L_k, the magnetizing inductance L_m, the input source V_{in}, the inductor L_3, the blocking voltage V_{C4}, and the clamped capacitor voltage V_{C2} are connected in series to provide energy to the output capacitor C_o and the load R. Meanwhile, capacitor C_3 keeps charging. The voltages across the diodes D_1 and D_2 are clamped by the windings of the coupled inductor and the clamped capacitors C_1 and C_2. Therefore, the voltage steps of diodes D_1 and D_2 are formed, and the voltage drops of the switches are obtained. The output diode current i_{Do} drops linearly. When the output diode D_o is reverse biased at t = t_8, this operating mode ends. When the switches are turned on, the new switching period begins.

2.2 Theoretical Analysis of Voltage Multiplier Converter

Voltage Gain Expression

When the proposed converter operates in the switching-on state, the following equations can be found in Fig. 3

$$V_{Lm} = kV_{in} \quad (1)$$

$$V_{Lk} = (1 - k)V_{in} \quad (2)$$

At modes V–VII, the energies of the leakage inductors are released to the capacitors C_1 and

C_2. According to the duty cycle of the released energy can be approximately obtained

$$D_o = 2(1 - D)/(N + 1) \quad (3)$$

By using the volt–second balance principle on the leakage inductance L_k and magnetizing inductor L_m, the voltages of L_k and L_m are found as

$$V_{Lm} = DkV_{in}/(1 - D) \quad (4)$$

$$V_{Lk} = D(1 - k)(N + 1)V_{in}/(2(1 - D)) \quad (5)$$

$$V_{N3} = NDkV_{in}/(1 - D) \quad (6)$$

The voltages of capacitors C_1, C_2, C_3, and C_4 can be expressed as

$$V_{C3} = NDV_{in}/(1 - D) \quad (7)$$

$$V_{C1} = V_{C2} = V_{Lk} + V_{Lm}$$

$$= (VinD((1 - k) + N(1 - k)))/2(1 - D) \quad (8)$$

$$V_{C4} = V_{in} + V_{C1} + V_{C3} + V_{N3} \quad (9)$$

Accordingly, collecting the terms, the voltage gain can be expressed as

$$G_k = \frac{V_o}{V_{in}} = \frac{V_{c1}+V_{c2}+V_{c3}+V_{c4}+V_{in}}{V_{in}}. \quad (10)$$

$$G = \frac{V_o}{V_{in}} = \frac{2+N}{1-D} + \frac{D(N+1)}{1-D} \quad (11)$$

Voltage Stress and Current Stress Expression

According to the above analysis, the voltage stresses on the power devices are given as follows:

$$V_{S1} = V_{S2} = V_{D1} = V_{D2} = \frac{V_{in}}{1-D} = \frac{V_O}{2+N+(N+1)D} \quad (12)$$

$$V_{D4} = \frac{NV_{in}}{1-D} = NV_O/2 + N + (N + 1)D \quad (13)$$

$$V_{D3} = V_{D0} = \frac{(N+1)V_{in}}{1-D} = (N + 1)V_0/(2 + (N + 1)D) \quad (14)$$

During the time interval [t_2, t_8], the on-state currents of the diodes D_0, D_1 and D_2 can be expressed as

$$I_{D0(t_2,t_8)} = I_0/1 - D \quad (15)$$

$$I_{D1(t_2,t_7)} = I_{D2(t_2,t_7)} = I_0/D_C \quad (16)$$

Then, based on the capacitor charge balance, during the time interval [t_0, t_2], the average current of capacitor C_1 can be written as

$$I_{C1[t_0,t_2]} = I_0/D \quad (17)$$

Hence, the currents of secondary side N_3 of the coupled inductor can be obtained as

$$I_{N3[t_0,t_2]} = I_0/D \quad (18)$$

$$I_{N3[t_2,t_8]} = I_0/(1 - D) \quad (19)$$

During the time interval [t_2,t_8], while using KCL at points of the primary side N_1 of the coupled inductor , diode D_1 and capacitor C_4 , the current of the leakage inductor can be expressed as

$$I_{L_{k[t_2,t_8]}} = (N + 3)I_0/(2(1 - D) \quad (20)$$

Duty Ratio

In order to show how different duty cycle and parasitic parameters influence the efficiency, some parameters are assumed in the following three cases.

Case I: R_L =0.02 Ω, N_1 =2, R_{DS} =0.075 Ω, R_D =0.05 Ω, R = 200 Ω, V_D =0.8V, V_{in} =20V.

Case II: R_L =0.04 Ω, N_1 =2, R_{DS} =0.075 Ω, R_D =0.05 Ω, R = 200 Ω,V_D =0.8V, V_{in} =20V.

Case III: R_L =0.06 ΩN_1 =2, R_{DS} =0.075 Ω, R_D =0.05 Ω, R = 200 Ω,V_D =0.8V, V_{in} =20V.

3 SIMULATION RESULTS

3.1 Open Loop System

The below converter is an open loop system with dual switches, three-winding

coupled inductor and voltage multiplier cells by achieving high output gain to a limited value.

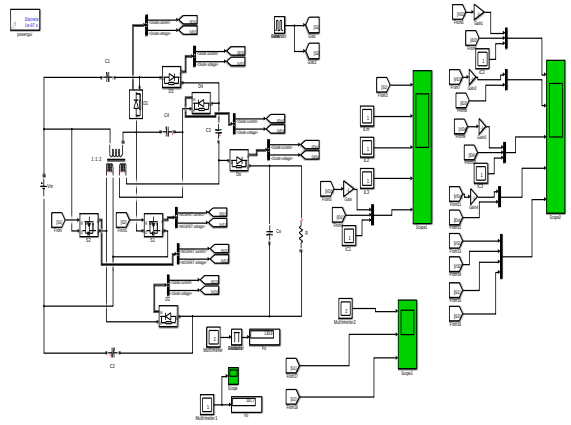

Fig.10 MATLAB simulation of voltage multiplier converter with coupled inductor without controller (Open Loop System)

Principle of Operation

Here, the converter consists of two active switches, five diodes and five capacitors. The two switches share same operation signal and one control circuit is needed. The input voltage is maintained at 20V and the duty ratio is varied giving constant output voltage as 200V.

Experimental Results

The following waveforms shows the output voltage at 200V with 20V as input maintaining the duty ratio at 0.5

Fig.11 Comparison of input and output voltage of 200V

Output Voltage comparison with Different Duty Ratio

In the below Table I, the value of output voltage changes as the duty ratio is varied, here, the duty ratio is varied manually giving different output voltages with constant input voltage of 20V.

Table I

Comparison with Different Duty Ratio

S.No	Input Voltage	Duty Ratio	Output Voltage
1	20	0.4	162
2	20	0.5	204
3	20	0.6	263
4	20	0.7	349

The input voltage is kept constant at 20V, the output voltage varies as the duty ratio is varied manually. As the maximum duty ratio will be less than 1, the maximum value to the output voltage would be approximately 530V.

3.2 Closed Loop System with PI Controller

Here comparison of error and change in error signals are to be made and gives the controlled output is measured by scope.

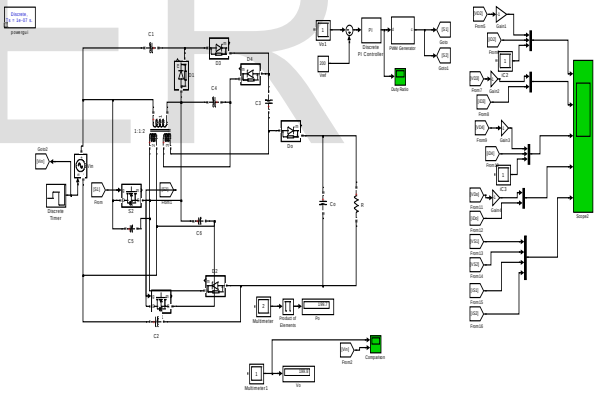

Fig.12 MATLAB simulation of voltage multiplier converter with coupled inductor with PI controller

Principle of Operation of PI controller

Here the input voltages are given as 10V, 15V, 20V, 25V, 30V, 40V and Reference voltage is given as 200V, these two inputs are given to the PI Controller. Comparison of the actual output voltage and reference voltage is carried out by using Error controller. It compares the error and change in error value and gives the controlling output voltage.

Simulation Experimental Results

The following waveforms shows the comparison between the input and output voltage with reference voltage. Here, we discuss different cases of the variation in duty ratio for different reference value.

In the below table, the desired value of the output voltage is achieved as the duty ratio is varied, here, the duty ratio is automatically varied giving different output voltages with variable input voltages.

TABLE II
For Reference Voltage = 200V

Variable input voltage	Output Voltage(Volts)	Output Power(Watts)
[20 25 15 30]	199	197.5

The above table shows the values of variable input voltages at a reference voltage of 200v maintaining the output voltage at 199V, in this the duty varies automatically.

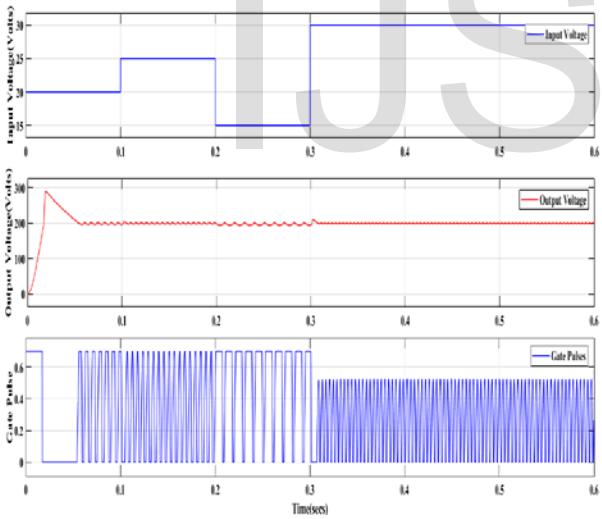

Fig.13 Waveforms of the Constant Output Voltage with varying Duty Ratio

TABLE III
For Reference Voltage = 360v

Variable input voltage	Output Voltage(Volts)	Output Power(Watts)
[20 25 30 40]	366.6	671.8

The above table shows the values of variable input voltages at a reference voltage of 360v maintaining the output voltage at 366.6V, in this the duty varies automatically.

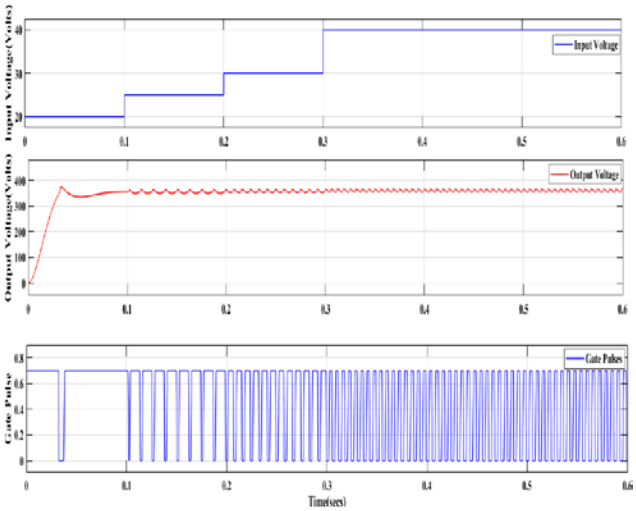

Fig.14 Waveforms of the Constant Output Voltage with varying Duty Ratio

The above figures (Fig.13 & Fig.14) and shows the automatic variation of duty ratio giving a constant output voltage.

4 COMPARISON WITH PREVIOUS CONVERTERS

Table IV shows the performance and comparison for the proposed converter and cascade boost converter. The number of diodes and capacitors are more than that in the cascade boost converter. However, the voltage stress of the active switch in cascade boost converter is equal to the output voltage, wherein, the voltage stress of the switch in proposed converter is very less than the output voltage. This makes the low on-resistance MOSFET available hence improving the efficiency. With the help of the controller, as the duty ratio increases, the voltage gain in the converter is far more than that in cascade boost converter.

TABLE IV
Comparison among different Converters

Topology	Cascade Boost Converter	Proposed Converter
No. of Active Switches	1	2
No. of Diodes	3	5
No. of	2	5

Capacitors		
Voltage Gain	$1/(1-D)^2$ =0.04	(2+N+D(N+1))/ (1-D) =11
Voltage stress of active switches	Vo = 200v	Vo/(2+N+(N+1) D)= 44.45v

The proposed circuit maintains the output voltage constantly with the variable input voltage by employing the PI controller which controls the output voltage by controlling the width of the triggering pulses or switching signals. The output response with the variable input voltage is represented in the Fig.15. Initially, during the transient time the output voltage increases up to maximum value and with the control action of the PI controller the desired output voltage is attained around 0.06 to 0.07secs. The Fig.14 represents comparison of input and output voltage with the reference voltage as 200V. The desired output voltage can be varied and is obtainable with the PI control strategy with the proposed circuit.

The control action of PI controller is represented in Fig.13 in the form of gate pulses. From the simulation result, it can be observed that the gate pulses are being varied with PI control to achieve desired output voltage.

5 CONCLUSION

The Simulation experimental results have been presented for a coupled inductor based DC-DC converter. The implementation of high step-up voltage conversion with automatic variation of duty ratio, voltage clamping feature and by turns ratio of the coupled inductor. The output voltage is compared with the reference value and the error is fed to PI Controller generating dynamic duty ratio. So, as compared with cascaded boost converters, here the duty ratio is automatically varied giving constant output voltage for any given constant value of the input voltages. The output voltage is as the user-defined value which is maintained constant.

REFERENCES

1.K.-C. Tseng, C.-C. Huang, and W.-Y. Shih, "A high step-up converter with a voltage multiplier module for a photovoltaic system," IEEE Trans.Power Electron., vol. 28, no. 6, pp. 3047–3057, Jun. 2013.

2.J. T. Bialasiewicz, "Renewable energy systems with photovoltaic power generators: Operation and modeling," IEEE Trans. Ind. Electron., vol. 55, no. 7, pp. 2752–2758, Jul. 2008.

3.Y. Xiong, X. Cheng, Z. J. Shen, C. Mi, H. Wu, and V. K. Garg, "Prognos-tic and warning system for power-electronic modules in electric, hybrid electric, and fuel-cell vehicles," IEEE Trans. Ind. Electron., vol. 55, no. 6, pp. 2268–2276, Jun. 2008.

4.K. Jin, X. Ruan, M. Yan, and M. Xu, "A hybrid fuel cell system," IEEETrans. Ind. Electron., vol. 56, no. 4, pp. 1212–1222, Apr. 2009.

5.W. Li and X. He, "Review of non-isolated high-step-up DC/DC converters in photovoltaic grid-connected applications," IEEE Trans. Ind. Electron., vol. 58, no. 4, pp. 1239–1250, Apr. 2011.

6.Z. Song, C. Xia, and T. Liu, "Predictive current control of three-phase grid-connected converters with constant switching frequency for wind energy systems," IEEE Trans. Ind. Electron., vol. 60, no. 6, pp. 2451–2464, Jun. 2013.

7.S. M. Chen, T. J. Liang, L. S. Yang, and J. F. Chen, "A safety enhanced, high step-up DC–DC converter for AC photovoltaic module application," IEEE Trans. Power Electron., vol. 27, no. 4, pp. 1809–1817, Apr. 2012.

8.Y. Zhao, W. H. Li, and X. N. He, "Single-phase improved active clamp coupled-inductor-based converter with extended voltage doubler cell," IEEE Trans. Power Electron., vol. 27, no. 6, pp. 2869–2878, Jun. 2012.

9.M. Prudente, L. L. Pfitscher, G. Emmendoerfer, E. F. Romaneli, and R. Gules, "Voltage multiplier cells applied to non-isolated DC–DC converters," IEEE Trans. Power Electron., vol. 23, no. 2, pp. 871–887, Mar. 2008.

10.A. Ajami, H. Ardi, and A. Farakhor, "A novel high step-up DC/DC con-verter based on integrating coupled inductor and switched-capacitor tech-niques for renewable energy applications," IEEE Trans. Power Electron., vol. 30, no. 8, pp. 4255–4263, Aug. 2015.

11.Y. Tang, D. J. Fu, J. R. Kan, and T. Wang, "Dual switches DC/DC converter with three-winding-coupled inductor and charge pump," IEEETrans. Power Electron., vol. 31, no.1, pp. 461–469, Jan. 2016.

12.G. V. Torrico-Bascope, R. P. Torrico-Bascope, D. S. Oliveira Jr., S.V. Araujo, F. L. M. Antunes, and C. G. C. Branco, "A high step-up converter based on three-state switching cell," in Proc. IEEE Int. Symp. Ind. Electron., 2006, pp. 998–1003.

13.W. Li, W. Li, X. Xiang, Y. Hu, and X. He, "High step-up interleaved converter with built-in transformer voltage multiplier cells for sustainable energy applications," IEEE

Trans. Power Electron., vol. 29, no. 6, pp. 2829–2836, Jun. 2014.